OMTM, Volume *17*

Supplemental Information

Intra-CSF AAV9 and AAVrh10 Administration in Nonhuman Primates: Promising Routes and Vectors for Which Neurological Diseases?

Karim Bey, Johan Deniaud, Laurence Dubreil, Béatrice Joussemet, Joseph Cristini, Carine Ciron, Juliette Hordeaux, Morwenn Le Boulc'h, Kevin Marche, Maud Maquigneau, Michaël Guilbaud, Rosalie Moreau, Thibaut Larcher, Jack-Yves Deschamps, Marion Fusellier, Véronique Blouin, Caroline Sevin, Nathalie Cartier, Oumeya Adjali, Patrick Aubourg, Philippe Moullier, and Marie-Anne Colle

Supplemental Information

Video S1: ICV contrast solution administration into right lateral ventricle in NHPs.

Figure S1: Focus on the ventral horns of thoracic and lumbar spinal cord of AAV-injected NHPs.

Longitudinal section of the thoracic **(A)** and lumbar **(B)** spinal cord of Mac 3 NHP injected with AAV9-GFP by LIT-KT injection demonstrating GFP expression across 5 mm. Scale bar = 1 mm. White hatched window into left panels picture represents the focus of the ventral horn presented into the right panels. Scale bar = 150 µm.

Figure S2: Transduced-cell type identification throughout spinal cord following AAV9 intra-CSF delivery.

AAV9 cell-specific tropism was determined in brain representative sections from NHPs injected by LIT-KT and ICV. Brain tissues were immunolabelled using Olig 2, GFAP, Iba1 and NeuN primaries for oligodendrocytes, astrocytes, microglial cells and neuron phenotyping, respectively, and an Alexa 555 (red channel)-coupled secondary antibody was used for cell detection. GFP was determined by native GFP fluorescence signal imaging (green channel). Main images show Alexa 555/GFP merged fluorescence signals. Scale bar = 100 µm. Hatched windows indicate regions with GFP-positive cells, and insets show higher magnification on cells harbouring both fluorescence signals: Alexa 555 (left) and GFP (right) channels. Scale bar = 25 µm.

Figure S3: Assessment of GFP specificity in NHP spinal cord and GFP-positive motor neurons quantification.

Confocal microscopy spectral images of the monkey ventral horn spinal cord were taken to determine the autofluorescence and native GFP fluorescence signal in the NHP spinal cord by using linear unmixing to separate native GFP spectra from autofluorescence spectra. To demonstrate the specificity with which GFP fluorescence is distinguished from autofluorescence, spectral imaging analysis was performed in **(A)** Mac 3 monkeys that received scAAV9-CBA-GFP. **(B)** The autofluorescence spectrum was determined by analysis of PBS-injected monkeys. Scale bar = 50 µm. **(C)** Graphical representation of the spectrum profile of the autofluorescence signal spectrum (O) and native GFP spectrum (■) demonstrating distinct emission wavelengths. **(D)** Quantification of ChAT/GFP colocalization in MN in cervical, thoracic and lumbar spinal cord of each NHP used in the study.

Figure S4: Brain analysed sections and GFP expression mapping.

(A) Representative macroscopic dissection of the NHP brain included in the study. GFP expression mapping was

performed in right hemisphere coronal sections 4, 16 and 23. Adapted from Colle et al. [10] **(B)** In coronal section 4, 25-µm cryosection was performed, and GFP expression was analysed by confocal microscopy in the frontal cortex (inset). In coronal section 16, GFP expression was analysed in the parietal cortex (inset 5), temporal cortex (inset 2), hippocampus (inset 1), body of caudate nucleus (inset 3), and putamen (inset 4). In coronal section 23, GFP expression was analysed in the fourth ventricle area of the brain stem (inset 1) and in the cerebellum (inset 2). Scale bar = 150 µm.

Figure S5: Histopathological examination of the cervical, thoracic and lumbar DRGs.

Haematoxylin, eosine and saffron staining were performed in cervical, thoracic and lumbar DRGs of all NHPs included in the study. Photomicrographs presented in the figure demonstrate representative histopathological lesions found in AAVrh10- and AAV9-LIT-KT-injected monkeys. Black arrows show mononuclear cell infiltration and black arrowhead point myelin digestion chambers in DRGs. Scale bar = 150 µm.

Figure S6: GFP expression in peripheral organs

GFP expression in peripheral organs following AAVrh10- and AAV9-LIT-KT and AAV9-ICV injection in NHP. Peripheral tissues were counter stained with 4',6-diamidino-2-phenylindole (DAPI) and native GFP expression was microscopically evaluated in the thymus, the spleen, the lung, the kidney, the jejunum and the testis. Scale bar = 150 µm (thymus – jejunum) and 50 µm (testis). White hatched windows represent the focus in one region of interest, presented into the left panels of each main photomicrograph. Scale bar = 50 µm (thymus – jejunum) and 10 µm.

Figure S7: GFP is expressed surrounding the Virchow-Robin space.

Representative confocal imaging was performed in injected NHPs brain 25-µm cryosection for the identification of the Virchow-Robin perivascular space and GFP expression in that same area. Endothelial cells and GFP are demonstrated by using red channels and green channels, respectively. Lumens of vessels are demonstrated by asterisks. Scale bar = 100 µm.

Table S1: Cellular and humoral immune responses against the GFP transgene.

			*IFN γ ELISPOT * [a]*		Anti-GFP IgG antibodies			
Animal identification	*Route*	*Capsid*	*PBMC*	*Splenocytes*	*d3*	*d7*	*d10*	*d Euth*
Mac 1	IT	10	+	+	*NA*	*NA*	*NA*	1/20480
Mac 2	IT	10	–	–	*nd*	*nd*	*nd*	*nd*
Mac 3	IT	9	+	–	*nd*	*nd*	*nd*	1/2560
Mac 4	IT	9	+	+	*nd*	*nd*	*nd*	1/2560
Mac 5	IT	9	–	–	*nd*	*nd*	*nd*	*nd*
Mac 6	IT	9	–	–	*nd*	*nd*	*nd*	1/163840
Mac 7	ICV	9	–	+	*nd*	*nd*	*nd*	*nd*
Mac 8	ICV	9	–	+	*nd*	*nd*	*nd*	*nd*

* GFP peptid pools; [a]: ELISPOT was performed at euthanasia time point; d: day; +: positive responder to GFP peptide pools
– : negative responder to GFP peptide pools; *NA*: not available sample; *nd*: not determine

Figure S1

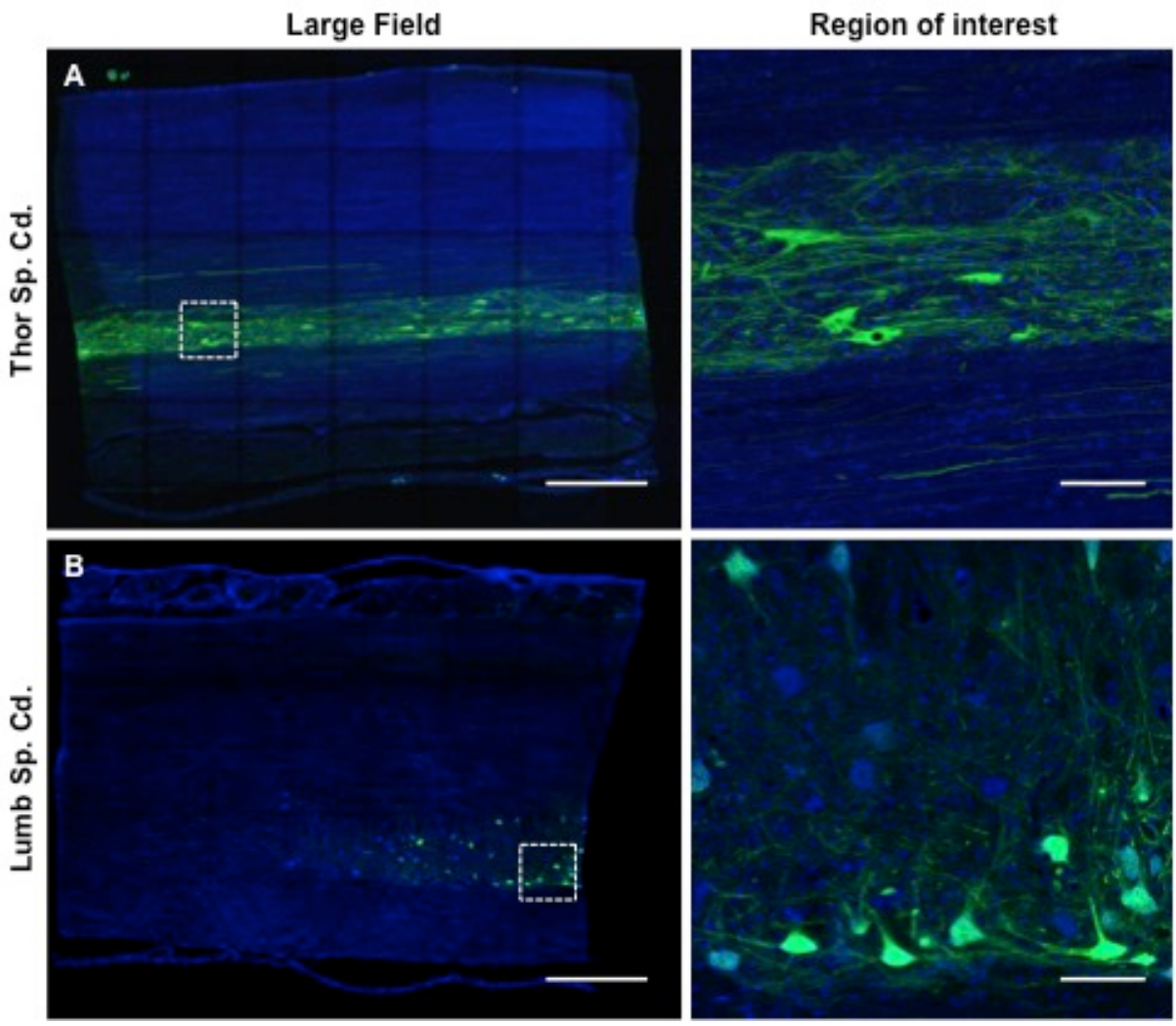

Figure S2

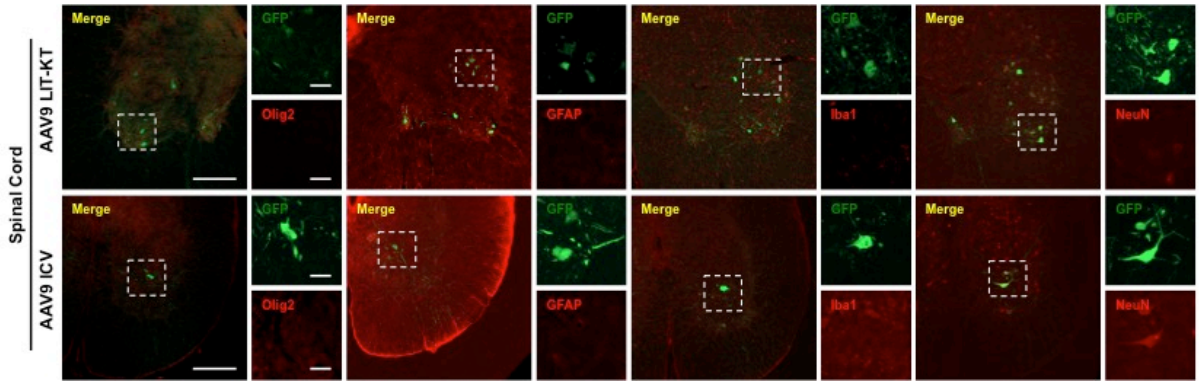
Spinal Cord
AAV9 LIT-KT
AAV9 ICV
Merge
GFP
Olig2
GFAP
Iba1
NeuN

Figure S3

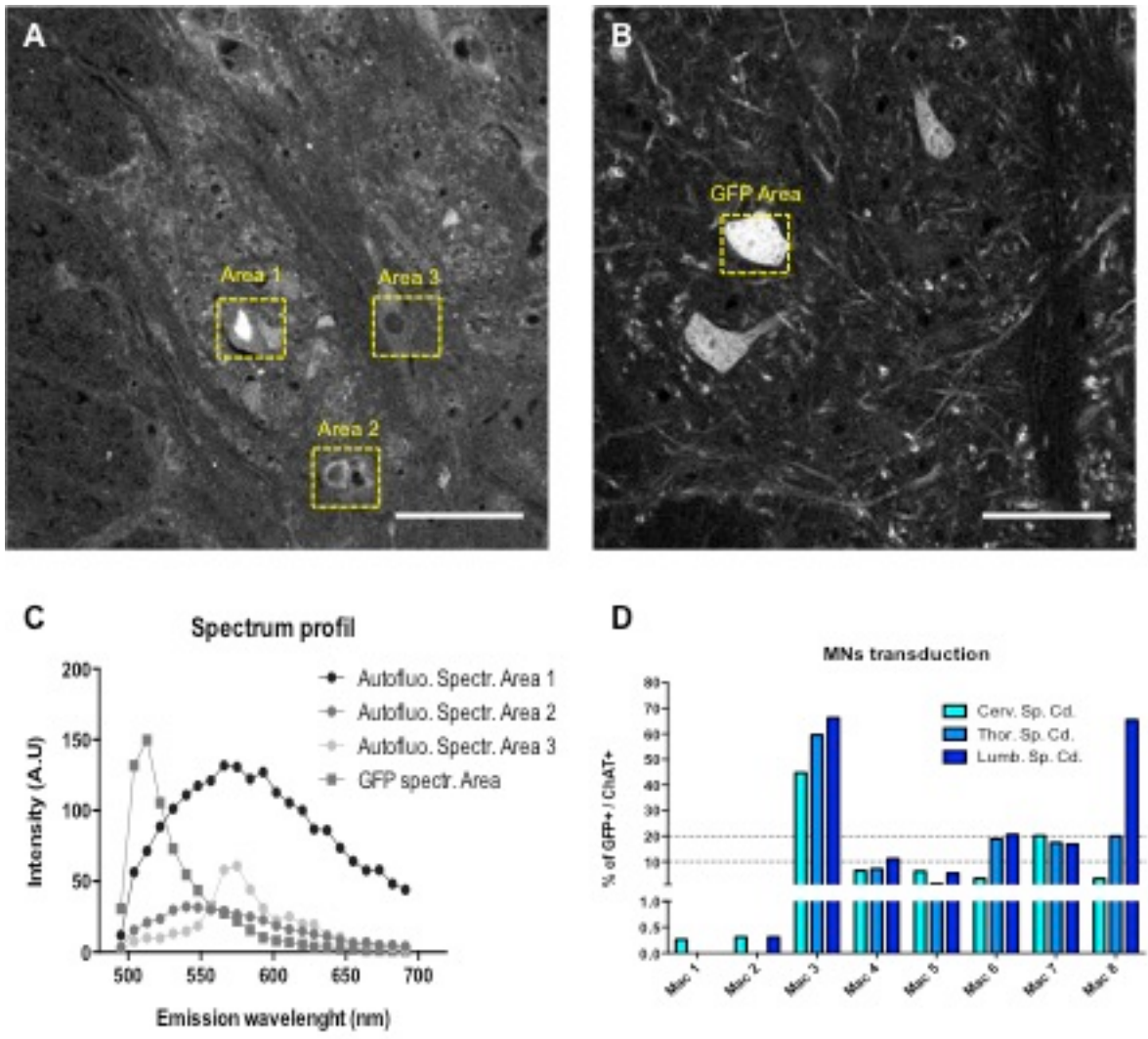
A
Area 1
Area 3
Area 2
B
GFP Area
C
Spectrum profil
Autofluo. Spectr. Area 1
Autofluo. Spectr. Area 2
Autofluo. Spectr. Area 3
GFP spectr. Area
Intensity (A.U)
Emission wavelenght (nm)
D
MNs transduction
Cerv. Sp. Cd.
Thor. Sp. Cd.
Lumb. Sp. Cd.
% of GFP+ / ChAT+

Figure S4

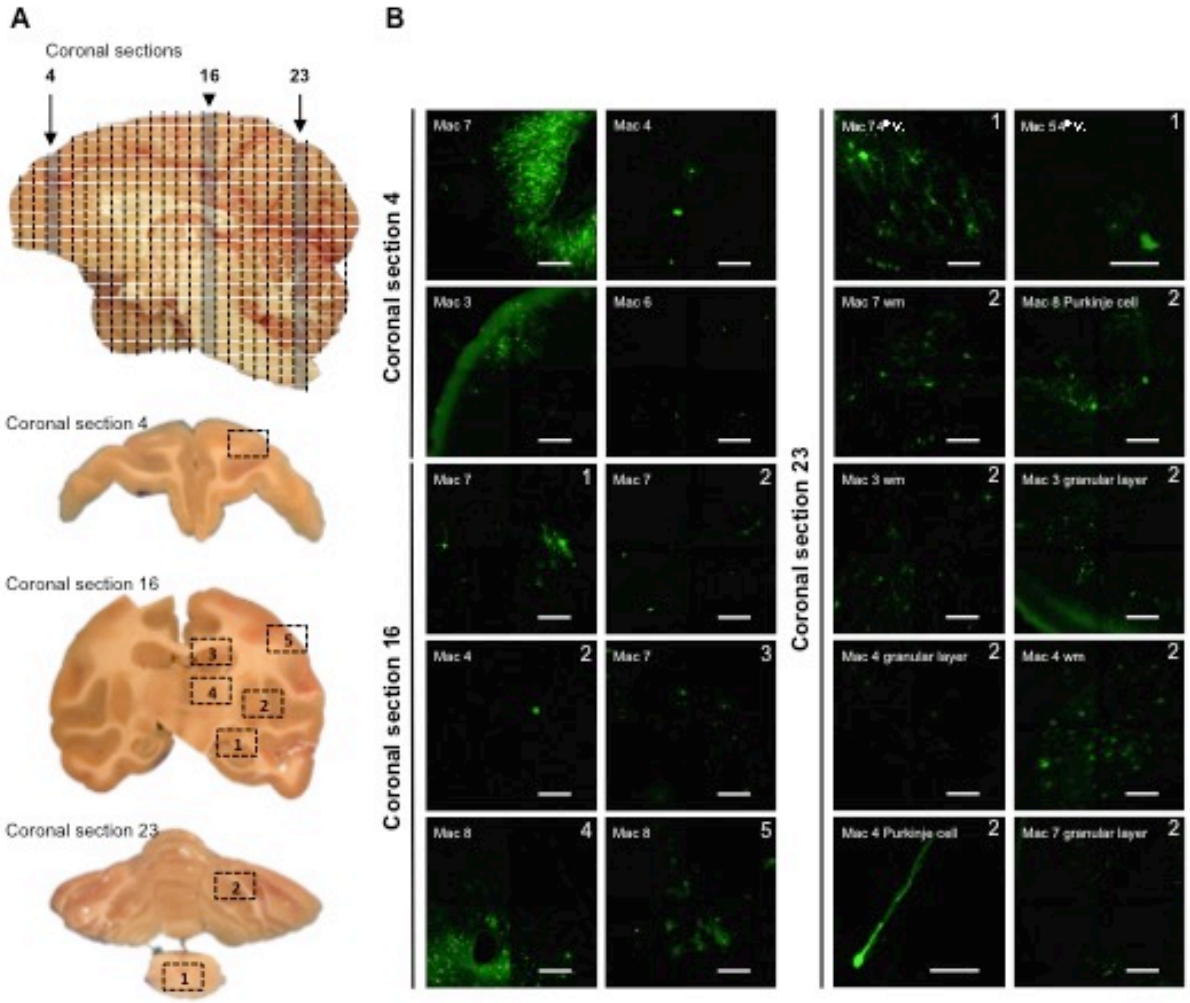
A
Coronal sections
4
16
23
Coronal section 4
Coronal section 16
Coronal section 23
B
Coronal section 4
Coronal section 16
Coronal section 23
Mac 7
Mac 4
Mac 3
Mac 6
Mac 7 1
Mac 7 2
Mac 4 2
Mac 7 3
Mac 8 4
Mac 8 5
Mac 7-PV. 1
Mac 5-PV. 1
Mac 7 wm 2
Mac 8 Purkinje cell 2
Mac 3 wm 2
Mac 3 granular layer 2
Mac 4 granular layer 2
Mac 4 wm 2
Mac 4 Purkinje cell 2
Mac 7 granular layer 2

Figure S5

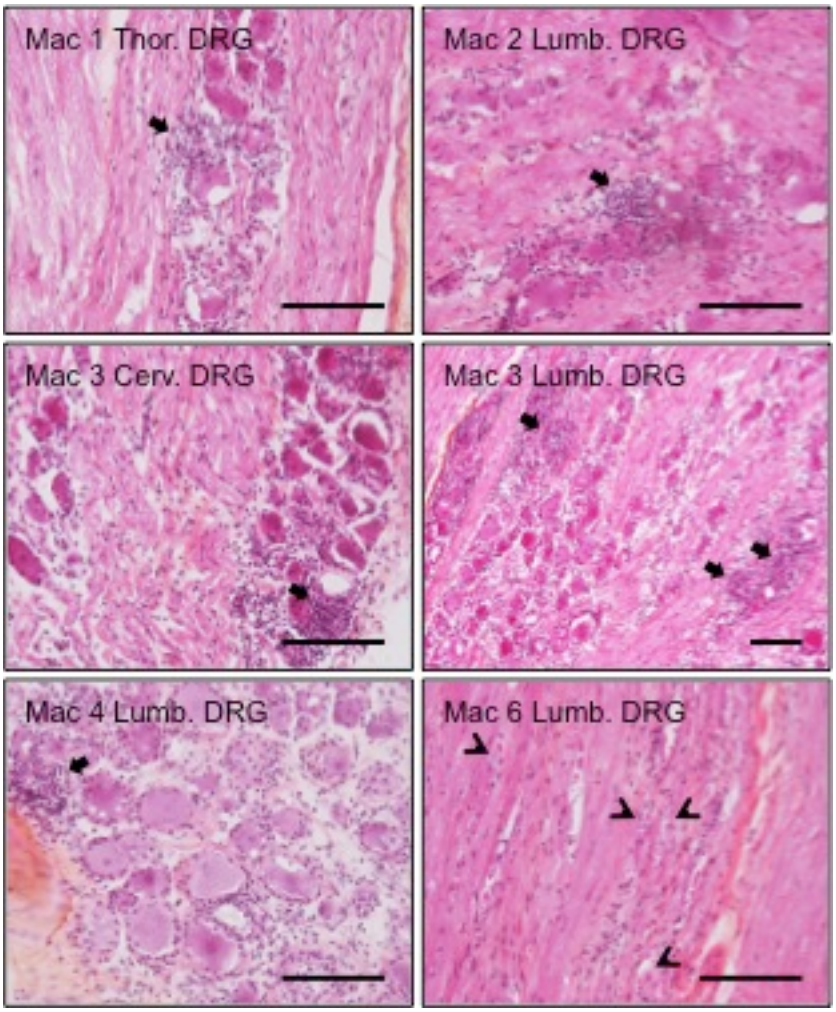
Mac 1 Thor. DRG
Mac 2 Lumb. DRG
Mac 3 Cerv. DRG
Mac 3 Lumb. DRG
Mac 4 Lumb. DRG
Mac 6 Lumb. DRG

Figure S6

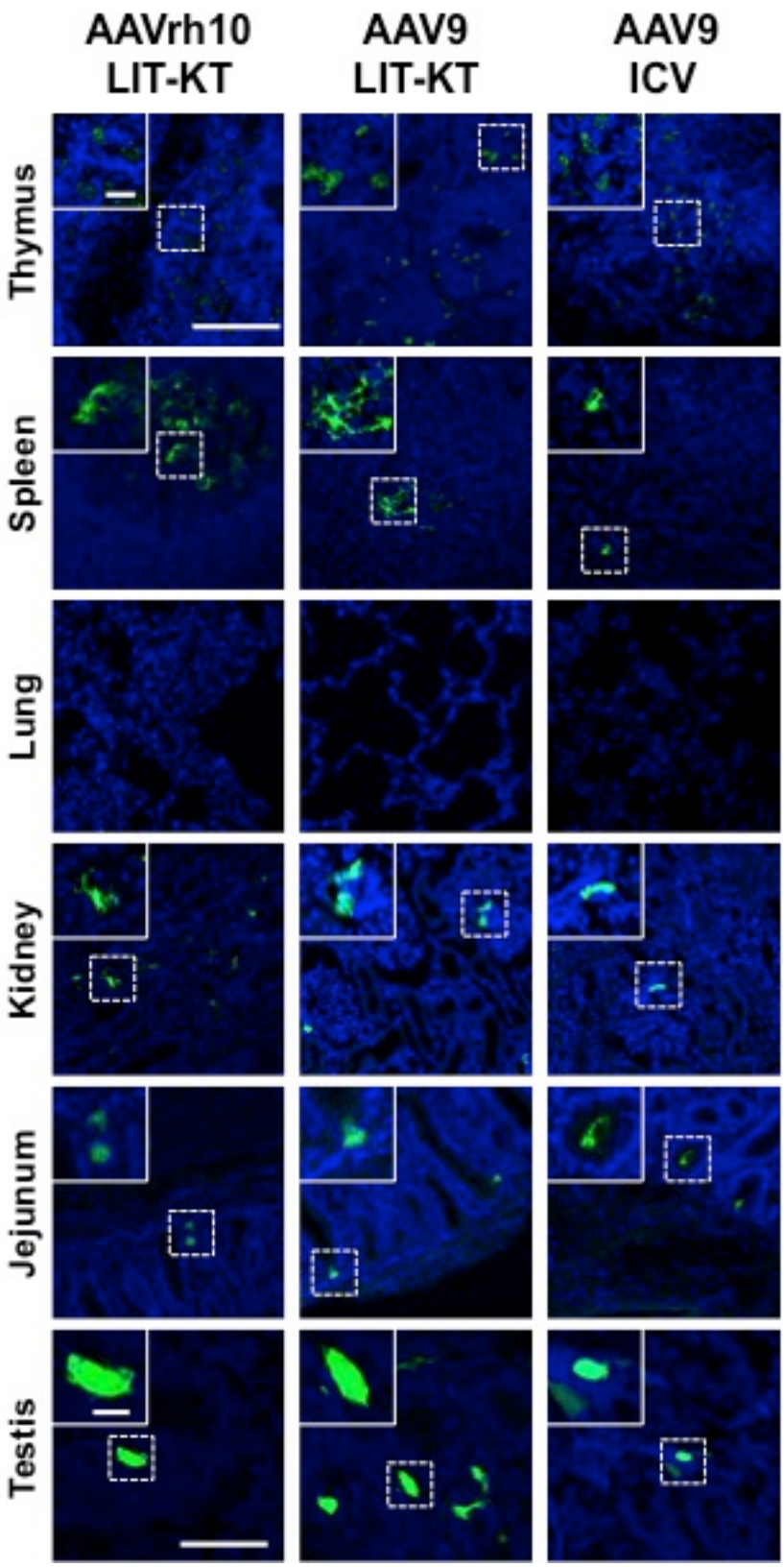
AAVrh10
LIT-KT
AAV9
LIT-KT
AAV9
ICV
Thymus
Spleen
Lung
Kidney
Jejunum
Testis

Figure S7

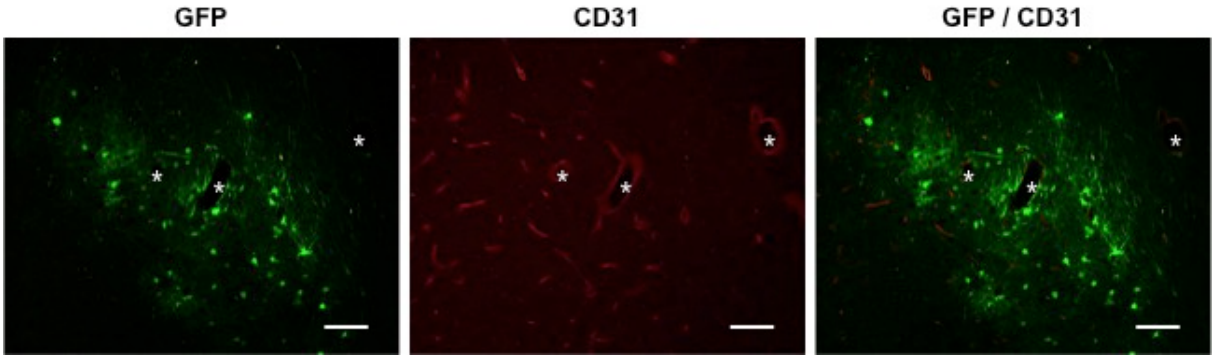

Video S1

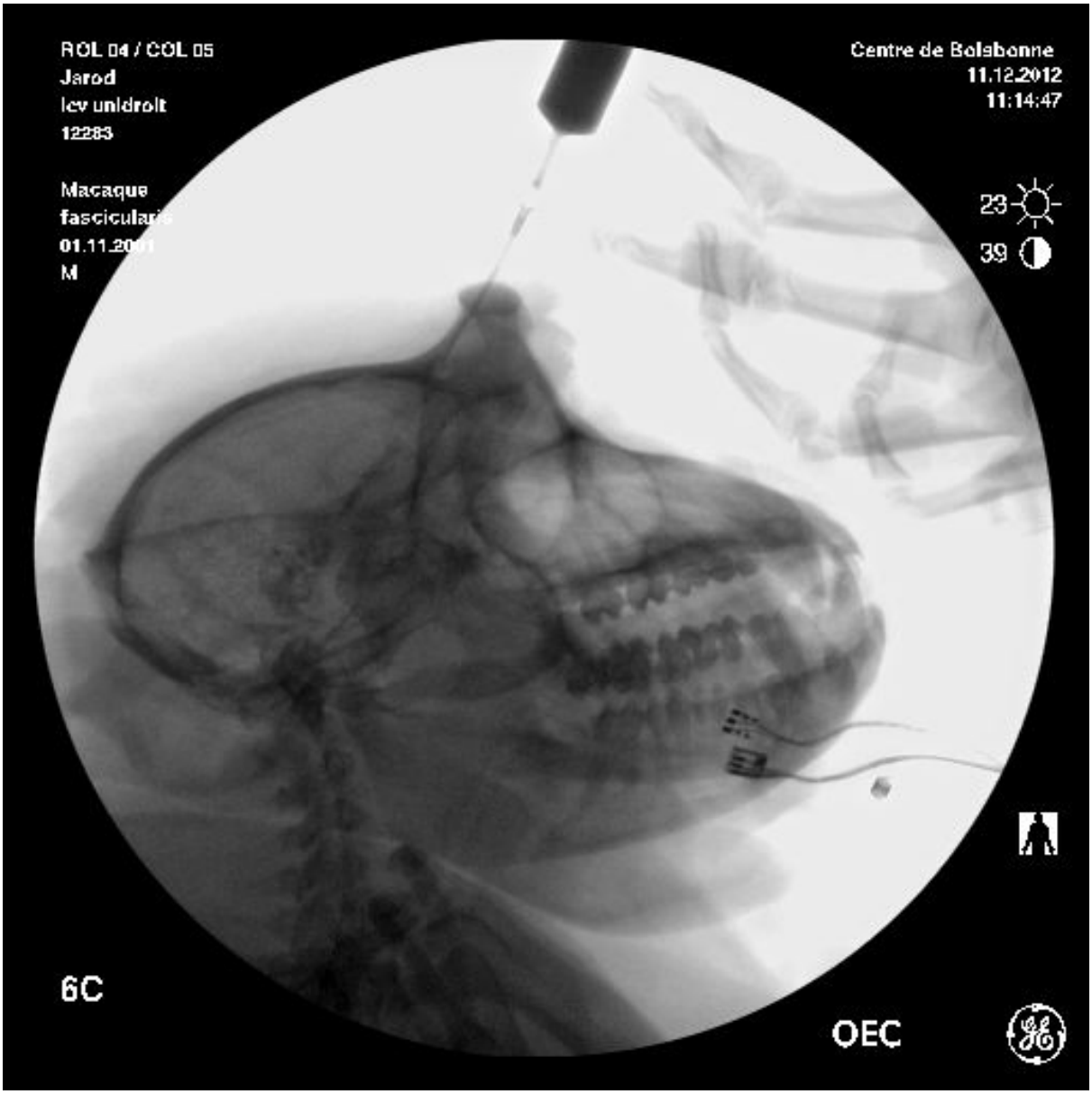
ROL 04 / COL 05
Jarod
lev unidroit
12283
Macaque
fascicularis
01.11.2001
M
Centre de Bolabonne
11.12.2012
11:14:47
23
39
6C
OEC

Supplemental Methods

Detection of anti-transgene humoral response

The presence of anti-GFP antibodies in primate sera was assessed by enzyme-linked immunosorbent assay (ELISA). Briefly, Nunc Maxisorp P96 plate (Thermo) was coated with 5 µg / mL of recombinant GFP protein (Merck). After an overnight incubation at + 4 °C, the wells were washed, saturated and incubated with two-fold dilutions of serum from 1/10 to 1/327,680. After 2 hours at 37 °C and a washing step, the wells were incubated for 1 hour at 37 °C with horseradish peroxidase (HRP)-conjugated anti-Rhesus immunoglobulin G (IgG, Southern Biotech). Signals were revealed using 2.2-3,3',5,5'-tetramethylbenzidine (TMB, Becton Dickinson) according to the manufacturer's recommendations. Absorbance was read at 450 nm with a correction at 570 nm on a Multiskan Go reader (Thermo). Threshold positivity was established from the mean of the optical density obtained for each dilution + 2SD from 22 negative sera obtained from naïve primates. IgG titers for experimental animals were defined as the highest serum dilution with an optical density that remained above the threshold.

Detection of the anti-transgene cellular response by using an interferon gamma (IFN-γ) enzyme-linked immunospot assay (ELISpot)

Briefly, peripheral blood mononuclear cells (PBMCs) collected at euthanasia were thawed and dispatched at 2E+5 cells into human anti-IFN-γ (MabTech) precoated polyvinylidene difluoride membrane Multiscreen® high throughput filter plates (Millipore). PBMCs were incubated with 5 peptide pools covering the GFP sequence (overlapping peptide library 15 per 10 mers; Sigma-Aldrich). Pools were replaced by culture medium alone for negative control or Concanavalin A for positive control. After 48 h of incubation at 37 °C in 5 % CO_2, the wells were washed and incubated with a biotinylated anti-IFN-γ antibody (clone 7-B6-1) MabTech and then with ExtrAvidin® alkaline phosphatase (Sigma Aldrich). The reaction was revealed using BCIP/NBT substrate (Thermo), spots were counted using an ELISpot Reader ELR07 (AID) and analysed with the AID ELISpot reader software v7.0. Only responses at least threefold higher than the negative control and above 50 spot-forming colonies per million cells were considered positive.